

LHC diphoton excess in a left-right symmetric model with minimal dark matter

Sanjib Kumar Agarwalla,^{1,*} Kirtiman Ghosh,^{2,†} and Ayon Patra^{3,4,‡}

¹ *Institute of Physics, Sachivalaya Marg, Sainik School Post, Bhubaneswar 751005, India*

² *Department of Physics and Astrophysics, University of Delhi, Delhi 110007, India*

³ *Institute of Convergence Fundamental Studies, Seoul National University of Science and Technology, Seoul 139-743, Korea*

⁴ *Regional Centre for Accelerator-based Particle Physics,
Harish-Chandra Research Institute, Jhansi, Allahabad - 211019, India**

We construct a model containing a viable dark matter candidate, in the framework of left-right symmetry, which can explain both width and cross-section of the observed 750 GeV diphoton excess at the LHC. We introduce a fermion quintuplet whose neutral component can be a possible dark matter candidate, whereas the charged components enhance the loop induced coupling of a 750 GeV singlet scalar with a pair of photons. We study the photo-production of the singlet scalar and its various decay modes, successfully addressing both the ATLAS and the CMS diphoton excess.

PACS numbers: 12.60.-i, 14.80.Bn, 14.80.Cp, 95.35.+d

At the intensity frontier, the ongoing Large Hadron Collider (LHC) experiment is expected to shed light on new physics scenarios to break apart our long-held understanding of the Standard Model (SM) of particle physics, and the recent tantalizing hint of a new resonance, giving rise to an excess in the diphoton invariant mass around 750 GeV, may be the first glimpse of that new physics [1–6]. This observed excess of diphoton events¹ at the early 13 TeV run of the LHC experiment [5, 6] could be explained as production of a new massive spin-0 or spin-2 resonance followed by its decay into a pair of photons. The most significant deviation from the SM background prediction was observed at $M_{\gamma\gamma} \sim 750$ (760) GeV by the ATLAS (CMS) collaboration. The 13 TeV ATLAS data with 3.2 fb^{-1} integrated luminosity indicates towards an excess in favor of a large width ($\Gamma \sim 45 \text{ GeV} \sim 0.06 M$) resonance, with a local significance of 3.9σ (3.6σ) in searches optimized for spin-0 (spin-2) hypothesis. For CMS collaboration with $\sqrt{s} = 13 \text{ TeV}$ and 3.3 fb^{-1} data, the local significance is maximized to 2.8σ (2.9σ) assuming spin-0 (spin-2) hypothesis for a resonance with $\Gamma \sim 10 \text{ GeV} \sim 0.014 M$. The best-fit values for the effective signal strength (namely, production cross-section times branching ratio to $\gamma\gamma$) of a 750 GeV resonance are $(5.5 \pm 1.5) \text{ fb}$ and $(4.8 \pm 2.1) \text{ fb}$ for ATLAS and CMS, respectively with 13 TeV data [7].

To explain this excess, a plethora of beyond the SM scenarios have been put forward in the literature (see Ref. [7] and the references therein). The obvious (and also maximally studied) explanation is a new spin-0 resonance (scalar or pseudoscalar) for which coupling to a pair of gluons/photons appears only at the loop level². Assuming gluon-gluon fusion to be the dominant production mechanism for the resonance, the observed signal cross-section requires additional colored and charged states. They need to have large coupling to the resonance to enhance its loop induced coupling to a pair of gluons/photons, which ultimately increases the production cross-section and diphoton decay width. Initial state gluons being colored objects are more prone to emit hadronic radiation (initial

state radiation, ISR) and thus, give rise to hadronic activity in the central region. Therefore, if gluon-gluon fusion is the production mechanism, the diphoton signal events are expected to be accompanied by a few ISR jets, which should have observable features in kinematical distributions like number of jets (n -jets) distribution, transverse momentum (p_T) distribution of diphotons *etc.* The ATLAS collaboration with limited luminosity has recently reported jet multiplicity distribution and diphoton p_T distribution in the diphoton excess region and its sideband [5]. In view of these distributions, it was already pointed out in Ref. [12, 13] that gluon-gluon fusion is slightly disfavored.

The other possible production mechanism for a 750 GeV scalar is the photo-production *i.e.*, production via photon-photon fusion [14–22]. Initial state photon being color singlet, the hadronic activity from ISR would be suppressed in photo-production, resulting in fewer central jets which is consistent with recent ATLAS observation [5]. The photo-production cross-section of a resonance (R) at the LHC can be estimated from its decay width into a pair of photons and parton distribution function of photon. The diphoton signal cross-section at LHC is given by [16]:

$$\sigma(R \rightarrow \gamma\gamma) = \sigma_0 \left(\frac{\Gamma_{\text{TOT}}}{\text{GeV}} \right) \text{Br}^2(R \rightarrow \gamma\gamma), \quad (1)$$

where Γ_{TOT} is the total decay width of resonance R and σ_0 is estimated³ to be around 240 fb [16] at the LHC with $\sqrt{s} = 13 \text{ TeV}$. Eq. 1 shows that large total decay width of resonance R and sizable (few %) branching ratio to diphoton could explain the cross-section and width of the observed diphoton excess.

The loop induced coupling of a scalar with a pair of photons is quadratically proportional to the charge of the particle inside the loop. In this work, we consider a minimal model [23, 24] for dark matter (DM) in the framework of $SU(3)_C \times SU(2)_L \times SU(2)_R \times U(1)_{B-L}$ gauge symmetry [25, 26], where B and L are baryon and lepton numbers respectively. Apart from the usual chiral fermions, scalar doublet, and bi-doublet required to break left-right (LR) symmetry, the particle spectrum includes an additional $SU(2)_R$ vector-like fermion quintuplet to accommodate a DM candidate (the neutral component of

¹ For a recent review on the main experimental, phenomenological, and theoretical issues related to the 750 GeV diphoton excess, see Ref. [7].

² Randall-Sundrum type graviton couples to a pair of gluons at tree-level and hence, could explain the excess as spin-2 resonance. However, in this case, it is non-trivial to suppress its decay to a pair of top-quarks or leptons since neither of them have been seen [8–11].

³ σ_0 gets contribution from fully inelastic ($\sim 63\%$), partially inelastic ($\sim 33\%$), and elastic ($\sim 4\%$) proton-proton scattering.

the quintuplet) and a singlet scalar to explain the LHC diphoton excess. The loop-induced diphoton decay width of the singlet scalar can be significantly enhanced due to multi-charged (depending on the $B-L$ charges) quintuplet fermions in the loop and hence, could potentially explain the LHC diphoton excess in totality. Before going into the details of diphoton signal cross-section and width of the signal distribution, we present our model briefly.

The matter content of this model along with their gauge quantum numbers in the framework of $G_{3221} \equiv SU(3)_c \times SU(2)_L \times SU(2)_R \times U(1)_{B-L}$ gauge symmetry are summarized in the following:

$$\begin{aligned} Q_L \left(3, 2, 1, \frac{1}{3} \right) &= \begin{pmatrix} u \\ d \end{pmatrix}_L, Q_R \left(3, 1, 2, \frac{1}{3} \right) = \begin{pmatrix} u \\ d \end{pmatrix}_R, \\ l_L (1, 2, 1, -1) &= \begin{pmatrix} \nu \\ e \end{pmatrix}_L, l_R (1, 1, 2, -1) = \begin{pmatrix} \nu \\ e \end{pmatrix}_R, \\ N (1, 1, 1, 0), \chi(1, 1, 5, 4) &= (\chi^{4+}, \chi^{3+}, \chi^{2+}, \chi^+, \chi^0)^T, \end{aligned}$$

where the Majorana fermion N is required for neutrino mass generation through inverse seesaw mechanism [27, 28], and χ is the vector-like fermion quintuplet under $SU(2)_R$ with a $B-L$ charge of 4. The minimal set of scalar multiplets⁴ [30, 31] required for the spontaneous breaking of G_{3221} to the SM, and then to $U(1)_{\text{EM}}$ are as follows:

$$H_R(1, 1, 2, 1) = \begin{pmatrix} H_R^+ \\ H_R^0 \end{pmatrix}, \Phi(1, 2, 2, 0) = \begin{pmatrix} \phi_1^0 & \phi_2^+ \\ \phi_1^- & \phi_2^0 \end{pmatrix}. \quad (2)$$

The $SU(2)_R \times U(1)_{B-L}$ breaks down to $U(1)_Y$ as the neutral component of H_R acquires a non-zero vacuum expectation value (VEV) denoted as $\langle H_R^0 \rangle = v_R$. On the other hand, VEVs of Φ namely, $\langle \phi_1^0 \rangle = v_1$ and $\langle \phi_2^0 \rangle = v_2$, are responsible for the electroweak (EW) symmetry breaking and for generation of the SM fermion masses and mixings. The electric charge Q is given as: $Q = T_L^3 + T_R^3 + Q_{(B-L)}/2$. In addition to the scalar doublet and bi-doublet in Eq. 2, we also introduce a singlet scalar $S(1, 1, 1, 0)$ to explain the LHC diphoton excess.

The structure of $SU(2)_L \times SU(2)_R \times U(1)_{B-L}$ breaking to $U(1)_{\text{EM}}$ introduces mixings between the gauge bosons of $SU(2)_L$, $SU(2)_R$, and $U(1)_{B-L}$ resulting in four massive (W_R , Z_R , and the SM W and Z -boson) and one massless (the SM photon) gauge bosons:

$$\begin{aligned} M_{W_R}^2 &= \frac{1}{2} g_R^2 (v_R^2 + v^2), \\ M_{Z_R}^2 &= \frac{1}{2} (g_R^2 + g_{B-L}^2) \left[v_R^2 + \frac{g_R^2 v^2}{(g_R^2 + g_{B-L}^2)} \right], \end{aligned} \quad (3)$$

where $v^2 = v_1^2 + v_2^2$ is the EW VEV ~ 174 GeV and $g_R = g_L = 0.653$. The left-handed W and Z boson masses are the same as in the SM with $g_Y = (g_R g_{B-L}) / (g_R^2 + g_{B-L}^2)^{1/2}$. The relevant couplings of the gauge bosons with χ are given as:

$$\begin{aligned} L \supset & - g_Y s_W Q \bar{\chi} Z^\mu \gamma_\mu \chi + e Q \bar{\chi} A^\mu \gamma_\mu \chi \\ & + \sqrt{g_R^2 - g_Y^2} \left[Q - \frac{g_R^2 Q_{B-L}}{2(g_R^2 - g_Y^2)} \right] \bar{\chi} Z_R^\mu \gamma_\mu \chi, \end{aligned} \quad (4)$$

⁴ For a study of various scalar sectors in the supersymmetric left-right scenario, see [29].

where $s_W = \sin \theta_W$ with θ_W being the Weinberg angle.

The quark and charged lepton masses are generated from the following Yukawa Lagrangian:

$$\begin{aligned} \mathcal{L}_Y &= Y^q \bar{Q}_L \Phi Q_R + \tilde{Y}^q \bar{Q}_L \tilde{\Phi} Q_R + Y^l \bar{l}_L \Phi l_R + \tilde{Y}^l \bar{l}_L \tilde{\Phi} l_R \\ &+ f_R \bar{l}_R \tilde{H}_R N + \frac{\mu_N}{2} N N + H.C. \end{aligned} \quad (5)$$

where Y and f are the Yukawa couplings and $\tilde{\Phi} = \tau_2 \Phi^* \tau_2$, $\tilde{H}_R = i \tau_2 H_R^*$. The quark and charged lepton masses in this model would then be given as:

$$\begin{aligned} M_u &= Y^q v_1 + \tilde{Y}^q v_2, M_d = Y^q v_2 + \tilde{Y}^q v_1, \\ M_l &= Y^l v_2 + \tilde{Y}^l v_1, \end{aligned} \quad (6)$$

while the neutrino masses are generated through the inverse seesaw mechanism. For simplicity, we will choose a large $\tan \beta (= v_1/v_2)$ limit which requires $Y_{33}^q \sim 1$ to explain the top mass while $\tilde{Y}_{33}^q < 10^{-2}$.

The scalar sector consists of a bidoublet field, an $SU(2)_R$ doublet field, and a real singlet. The most general scalar potential involving these fields is given by:

$$\begin{aligned} V_H \supset & -\mu_1^2 \text{Tr} [\Phi^\dagger \Phi] - \mu_2^2 \text{Tr} [\tilde{\Phi} \Phi^\dagger + H.C.] - \mu_R^2 H_R^\dagger H_R \\ & - \frac{\mu_S^2}{2} S^2 + \lambda_1 [\text{Tr} (\Phi^\dagger \Phi)]^2 + \lambda_4 \text{Tr} (\Phi^\dagger \Phi) \text{Tr} [\tilde{\Phi} \Phi^\dagger + H.C.] \\ & + \lambda_2 \left[\left\{ \text{Tr} (\tilde{\Phi} \Phi^\dagger) \right\}^2 + H.C. \right] + \lambda_3 \text{Tr} (\tilde{\Phi} \Phi^\dagger) \text{Tr} (\tilde{\Phi}^\dagger \Phi) \\ & + \alpha_3 \mu_3 S \text{Tr} (\Phi^\dagger \Phi) + \alpha_4 \mu_4 S \text{Tr} [\tilde{\Phi} \Phi^\dagger + H.C.] \\ & + \alpha_5 \mu_5 S H_R^\dagger H_R + \frac{\beta_1}{2} S^2 \text{Tr} (\Phi^\dagger \Phi) + \frac{\beta_2}{2} S^2 \text{Tr} [\tilde{\Phi} \Phi^\dagger + H.C.] \\ & + \frac{\beta_3}{2} S^2 H_R^\dagger H_R + \rho_1 H_R^\dagger H_R \text{Tr} [\Phi^\dagger \Phi] + \rho_3 H_R^\dagger \Phi \Phi^\dagger H_R \\ & + \rho_2 H_R^\dagger H_R \text{Tr} [\tilde{\Phi} \Phi^\dagger + H.C.] + \rho_4 H_R^\dagger \Phi^\dagger \Phi H_R \\ & + \lambda_R (H_R^\dagger H_R)^2 + A_S \mu_S S^3 + \frac{\lambda_S}{4} S^4. \end{aligned} \quad (7)$$

The Higgs spectrum of this model consists of four CP-even scalars, one CP-odd pseudoscalar, and one charged Higgs boson. Two CP-odd states, and two charged states are eaten up by the four massive gauge bosons. After diagonalizing the mass-squared matrix, one can easily obtain a light SM-like 125 GeV Higgs boson denoted by h , consisting almost entirely of the real part of ϕ_1^0 field. We also get a 750 GeV scalar denoted by H_1 , consisting of almost purely the singlet S with negligible mixing with the others. Two very heavy states H_2 and H_3 with masses of the order of v_R consisting of real part of ϕ_2^0 and H_R^0 states are also present in the spectrum. The heavy states are required to be heavier than 15 TeV in order to suppress flavor changing neutral currents [32–36]. This can be easily satisfied in our model by choosing a high value (> 10 TeV) for the right-handed symmetry breaking scale, v_R . Our model can accommodate the above mentioned scalar mass spectrum for a wide range of parameter choice. A typical set of parameters is given in Tab I as a benchmark point (BP). The mass of the pseudo-scalar A_0 and the charged Higgs boson H^\pm are also proportional to v_R , and hence, are heavier than 15 TeV.

The original motivation for introducing the vector-like quintuplet fermion $\chi(1, 1, 5, 4)$ was to obtain a candidate for DM [23]. The components of quintuplet are mass degenerate at tree-level, but radiative corrections remove this

Particle	Mass	Composition
h	125 GeV	$0.999\phi_1^0 + 0.029\phi_2^0 - 0.010S - 0.003H_R^0$
H_1	751 GeV	$0.010\phi_1^0 + 0.0002\phi_2^0 + 0.999S - 0.001H_R^0$
H_2	18.36 TeV	$0.020\phi_1^0 - 0.617\phi_2^0 + 0.001S + 0.787H_R^0$
H_3	18.43 TeV	$0.021\phi_1^0 - 0.787\phi_2^0 - 0.001S - 0.617H_R^0$

TABLE I: Scalar mass eigenstates for $\lambda_1 = 0.15$, $\lambda_2 = -0.35$, $\lambda_3 = 0.831$, $\lambda_4 = 0.01$, $\alpha_3 = 0.14$, $\alpha_4 = 0.1$, $\mu_3 = 174$ GeV, $\mu_4 = 174$ GeV, $\beta_1 = 0.1$, $\beta_2 = 0.1$, $\beta_3 = 0.004$, $\rho_1 = 0.2$, $\rho_2 = 0.2$, $\rho_3 = 1$, $\rho_4 = 1$, $\mu_S = 340$ GeV, $v_1 = 173.9$ GeV, $v_2 = 5$ GeV.

degeneracy. The mass splitting due to quantum corrections is given by,

$$M_{\chi^Q} - M_{\chi^0} = \frac{g_R^2}{(4\pi)^2} M \left[Q(Q - Q_{B-L}) f(r_{W_R}) - Q \left(\frac{g_Y^2}{g_{B-L}^2} Q - Q_{B-L} \right) f(r_{Z_R}) - \frac{g_Y^2}{g_R^2} Q^2 \{ s_W^2 f(r_Z) + c_W^2 f(r_\gamma) \} \right], \quad (8)$$

where $r_X = m_X/M$ and $f(r) \equiv 2 \int_0^1 dx (1+x) \log[x^2 + (1-x)r^2]$. The masses of the charged components of the quintuplet get positive contribution from the radiative corrections and hence, χ^0 becomes the lightest among the quintuplet fermions. Being weakly interacting and lightest member of the quintuplet, χ^0 could be a good candidate for dark matter. The stability of χ^0 is ensured by its gauge quantum numbers. Being a part of the quintuplet, χ^0 can decay to the SM particles via interactions with dimension-6 or higher operators and thus, its decay width is suppressed atleast by a factor of $1/\Lambda^2$. For a TeV scale χ^0 , the decay width via dimension-6 operator is of the order of M^3/Λ^2 which corresponds to a lifetime greater than the age of the universe for $\Lambda \gtrsim 10^{14}$ GeV.

In this work, we consider the scalar H_1 , which is dominantly singlet, as a candidate for the 750 GeV diphoton resonance observed at the LHC. Being singlet, H_1 has Yukawa interaction only with the quintuplet fermion. It has also couplings (arising from the scalar potential) with a pair of Higgs and other heavy scalars. The relevant interactions for collider phenomenology related to H_1 are given by:

$$L_S \supset \alpha_3 \mu_3 H_1 hh + \lambda_\chi \bar{\chi} \chi H_1, \quad (9)$$

where λ_χ is the Yukawa coupling, α_3 is a dimensionless parameter, and μ_3 is a parameter with a dimension of mass. Therefore, apart from its mass (m_{H_1}), the collider phenomenology of H_1 depends on μ_3 which we choose to be equal to the EW VEV (174 GeV), α_3 and λ_χ .

The dominant decay modes of H_1 are its tree level decay into a pair of SM Higgs or a pair of quintuplet fermions (if kinematically possible). H_1 can also decay into a pair of photons or pair of Z -bosons or $Z\gamma$ pairs via loops involving quintuplet fermions. The loop induced decay into photons is quartically proportional to the electric charge of the loop fermion. Therefore, in presence of multi-charge quintuplet fermions in the loop, the decay width of H_1 into a pair of photons gets enhanced by orders of magnitude in our model. This motivates us to study the diphoton signature of H_1 produced via photon-photon fusion at the LHC. It was shown in Eq. 1 that the diphoton signal cross-section depends on the total decay width (Γ_{TOT}) and the branching ratio into $\gamma\gamma$ of H_1 . The decay widths for different

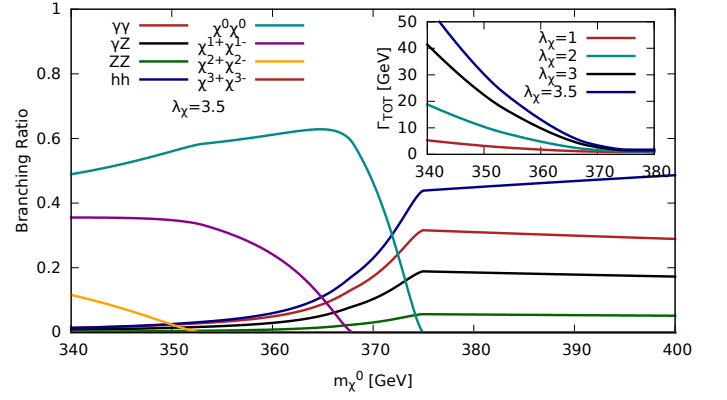


FIG. 1: Branching ratios of H_1 into different decay modes as a function of mass of χ^0 for a fixed value of $\lambda_\chi = 3.5$. Inset shows the total decay width of H_1 as a function of m_{χ^0} for different values of λ_χ .

decay channels are given by,

$$\begin{aligned} \Gamma_{hh} &= \frac{\alpha_3^2 \mu_3^2}{8\pi m_{H_1}} \left(1 - \frac{4m_h^2}{m_{H_1}^2} \right)^{\frac{1}{2}}, \\ \Gamma_{\chi_i \bar{\chi}_i} &= \frac{\lambda_\chi^2}{8\pi} m_{H_1} \left(1 - \frac{4m_{\chi_i}^2}{m_{H_1}^2} \right)^{\frac{3}{2}}, \\ \Gamma_{\gamma\gamma} &= \frac{\alpha^2 m_{H_1}^3 \lambda_\chi^2}{256\pi^3} \left| \sum_{\chi_i} \frac{Q_{\chi_i}^2}{m_{\chi_i}} A_{\frac{1}{2}} \left(\frac{m_{H_1}^2}{4m_{\chi_i}^2} \right) \right|^2, \\ \Gamma_{Z\gamma} &= \frac{\alpha^2 m_{H_1}^3 \lambda_\chi^2}{128\pi^3} \tan^2 \theta_W \left| \sum_{\chi_i} \frac{Q_{\chi_i}^2}{m_{\chi_i}} A_{\frac{1}{2}} \left(\frac{m_{H_1}^2}{4m_{\chi_i}^2} \right) \right|^2, \\ \Gamma_{ZZ} &= \frac{\alpha^2 m_{H_1}^3 \lambda_\chi^2}{256\pi^3} \tan^4 \theta_W \left| \sum_{\chi_i} \frac{Q_{\chi_i}^2}{m_{\chi_i}} A_{\frac{1}{2}} \left(\frac{m_{H_1}^2}{4m_{\chi_i}^2} \right) \right|^2, \end{aligned} \quad (10)$$

where $\chi_i \in \{\chi^{++++}, \chi^{+++}, \chi^{++}, \chi^+, \chi^0\}$. m_{χ_i} and Q_{χ_i} are the mass and charge of the corresponding χ_i respectively. The loop function $A_{1/2}(x)$ is given by, $A_{1/2}(x) = 2x^{-2} [x + (x-1)f(x)]$, where, $f(x) = -[\ln\{(1+\sqrt{1-x})/(1-\sqrt{1-x})\} - i\pi]^2/4$ for $x > 1$ and $f(x) = \arcsin^2 \sqrt{x}$ for $x \leq 1$. Eqs. 10 shows that the total decay width and hence, the branching ratios crucially depend on the masses of the quintuplet fermions. In order to calculate the masses of quintuplet fermions which depend on the masses of W_R and Z_R (see Eq. 8), we assume $v_R = 13.0$ TeV which corresponds to $m_{W_R} = 6.0$ TeV and $m_{Z_R} = 7.2$ TeV. In Fig. 1, we show the branching ratios of H_1 into different decay modes as a function of χ^0 mass denoted by m_{χ^0} for a fixed value of $\lambda_\chi = 3.5$. The inset of Fig. 1 depicts the total decay width as a function of m_{χ^0} for different values of λ_χ . Fig. 1 clearly demonstrates that H_1 dominantly decays into a pair of quintuplet fermions if the decay is kinematically possible and the total decay width is quite large in this case (see the inset). If the decay to $\chi_i \bar{\chi}_i$ is forbidden then the dominant decay mode is a pair of the SM Higgs bosons where the decay to diphoton being the second dominant mode.

The large decay width and significant branching ratio into a pair of photons in Fig. 1 for $m_{\chi_i} < m_{H_1}/2$ indicates towards the possibility of explaining the cross-section and width of LHC diphoton excess via the photo-production of H_1 and followed by its decay into $\gamma\gamma$. In Table II, we have presented our numerical results for three different

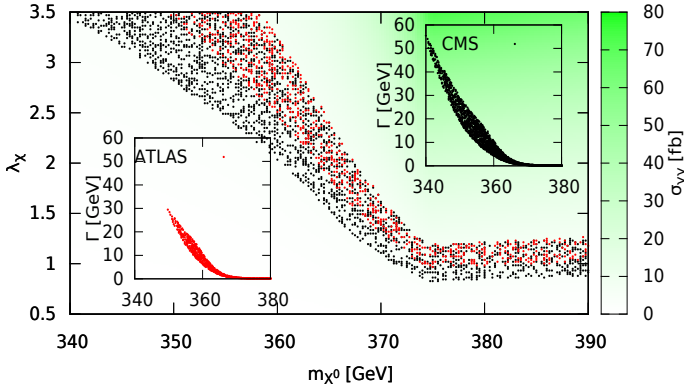


FIG. 2: Cross-section for the 750 GeV resonance decaying into diphoton is presented by color gradient as a function of DM-mass (m_{χ^0}) and Yukawa coupling (λ_χ). The red and black dotted regions correspond to the cross-sections consistent with the observed diphoton excess at the ATLAS and CMS detectors, respectively. The total decay width of the 750 GeV resonance for red and black dotted points are shown in the inset.

benchmark points defined by λ_χ and m_{χ^0} . Table II contains quintuplet mass spectrum, relevant decay widths (including the total decay width), and diphoton signal cross-section at the 13 TeV LHC for a H_1 with 750 GeV mass. It also shows that the chosen BPs are consistent (both cross-section and width) with the LHC observed diphoton excess. In Fig. 2, we have shown our model prediction for the diphoton cross-section by color gradient for a scan over the parameter space defined by m_{χ^0} (along x-axis) and λ_χ (along y-axis). We also indicate the region of parameter space consistent with the ATLAS and CMS measured excess by red and black dots, respectively. The total decay width corresponding to the red and black dots are depicted in the insets of Fig. 2. There is a large region of parameter space in our model that gives a diphoton signature which is consistent with the LHC observed excess in totality (*i.e.*, both the cross-section and width of the excess).

Finally, we arrive at a discussion on the present bounds (from collider as well as DM experiments), and future confirmatory tests for our model. The explanation for the cross-section and width of LHC diphoton excess requires the DM mass to be $\sim m_{H_1}/2$. Therefore, the DM annihilation cross-section is enhanced due to the resonant contribution from H_1 and hence, the upper bound on the DM relic density from WMAP/PLANK data [37, 38] can be easily satisfied in this particular part of parameter space. However, the large $B-L$ charge of the quintuplet results in an enhanced DM-nucleon scattering cross-section and hence, stringent constraints arise from direct DM detection experiments. χ^0 interacts with nucleon via exchange of a Z_R -boson and thus, the DM-nucleon cross-section is suppressed by $1/m_{Z_R}^4$. In Fig. 3, we give the χ^0 -proton

and χ^0 -neutron scattering cross-section as a function of m_{Z_R} . The experimental bound on DM-nucleon scattering cross-section depends on DM-mass. The shaded region (in the inset of Fig. 3) in $m_{DM}-m_{Z_R}$ plane is consistent with the LUX [39] upper bound on the DM-nucleon scattering cross-section. It also clearly shows that the DM-mass ~ 375 GeV is allowed for $m_{Z_R} \sim 7$ TeV.

At the LHC, the pair-production of quintuplet fermions take place via quark-antiquark (s -channel Z/γ^* -exchange) or photon-photon (t -channel) initial states. A quintuplet fermion decays into next lighter quintuplet fermion in as-

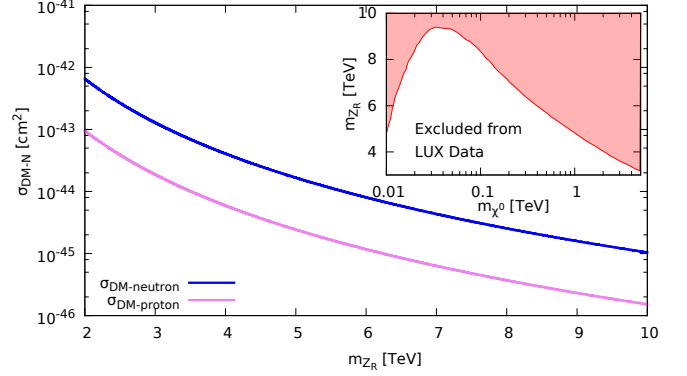


FIG. 3: χ^0 -proton and χ^0 -neutron scattering cross-section as a function of m_{Z_R} . In the inset, the shaded region in $m_{DM}-m_{Z_R}$ plane is consistent with the LUX [39] upper bound on DM-nucleon scattering cross-section.

sociation with a lepton-neutrino pair or quark-antiquark pair via tree-level 3-body decay involving an off-shell W_R^* . Though the cross-sections are suppressed, the pair-production of charged quintuplet fermions give rise to spectacular multi-lepton (4 same sign leptons (SSL), 3-SSL, 2-SSL, 8, 7, 6, 5 lepton *etc.*) signatures at the LHC. However, due to small mass splitting between the quintuplet fermions (see Table II), the resulting leptons are usually soft and fall below the minimum transverse momentum threshold required at the LHC for most of the events. A dedicated collider study is required to probe the spectacular leptonic signatures of our model.

To summarize, we have explained the the cross-section and width of both ATLAS and CMS diphoton excess by postulating a 750 GeV singlet scalar in the framework of a left-right model which also gives a viable candidate for DM in the form of the neutral component of an $SU(2)_R$ vector-like fermion quintuplet. The loop induced coupling of the 750 GeV scalar with $\gamma\gamma$ is enhanced by multi-charged quintuplet fermions. We have studied the photo-production of this scalar followed by its decay to $\gamma\gamma$ at the 13 TeV LHC. We have also discussed the bounds from the direct DM detection experiment such as LUX as well as future collider signatures of our proposed model.

λ_χ	m_{χ^0} GeV	$m_{\chi^{1+}}$ GeV	$m_{\chi^{2+}}$ GeV	$m_{\chi^{3+}}$ GeV	$m_{\chi^{4+}}$ GeV	$\sigma_{DM-n} \times 10^{45} [\text{cm}^2]$	$\sigma_{DM-p} \times 10^{46} [\text{cm}^2]$	$\sigma_{LUX} \times 10^{45} [\text{cm}^2]$	$\Gamma_{\gamma\gamma}$ GeV	$\Gamma_{Z\gamma}$ GeV	Γ_{ZZ} GeV	Γ_{hh} GeV	Γ_{TOT} GeV	$\sigma_{\gamma\gamma}$ fb
3.51	349.0	357.2	374.1	399.8	434.1	3.9	5.7	4.2	0.73	0.43	0.13	0.78	31.9	4.0
2.52	355.0	363.3	380.5	406.4	441.2				0.35	0.21	0.06	0.78	11.1	2.7
1.99	374.0	382.7	400.5	427.4	463.4				0.18	0.11	0.03	0.78	1.15	7.1

TABLE II: Quintuplet fermions mass spectrum, DM-neutron, DM-proton scattering cross-sections, and corresponding LUX [39] bound, decay width of 750 GeV singlet scalar into $\gamma\gamma$, $Z\gamma$, ZZ , hh as well as total decay width and diphoton cross-section at 13 TeV LHC are shown for three benchmark points defined by λ_χ and DM-mass (m_{χ^0}). We consider $g_R/g_L = 1.0$ and $m_{Z_R} = 7.2$ TeV.

Acknowledgments

S.K.A. is supported by the DST/INSPIRE Research Grant [IFA-PH-12], Department of Science & Technology, India. The work of K.G. is supported by an Inspire Faculty Fellowship from the Government of India, at the University of Delhi. A.P. is currently visiting Harish-Chandra Research Institute (HRI) and would like to thank the Regional Centre for Accelerator-based Particle Physics, HRI for hospitality during the visit, when part of this work was done. We would also like to thank Prof. Kaladi Babu for useful discussions.

* Electronic address: sanjib@iopb.res.in

† Electronic address: kirti.gh@gmail.com

‡ Electronic address: ayon@okstate.edu

- [1] T. A. collaboration, “Search for resonances decaying to photon pairs in 3.2 fb^{-1} of pp collisions at $\sqrt{s} = 13 \text{ TeV}$ with the ATLAS detector,” (2015).
- [2] C. Collaboration (CMS), “Search for new physics in high mass diphoton events in proton-proton collisions at 13TeV ,” (2015).
- [3] T. A. collaboration, “Search for resonances in diphoton events with the ATLAS detector at $\sqrt{s} = 13 \text{ TeV}$,” (2016).
- [4] C. Collaboration (CMS), “Search for new physics in high mass diphoton events in 3.3 fb^{-1} of proton-proton collisions at $\sqrt{s} = 13 \text{ TeV}$ and combined interpretation of searches at 8 TeV and 13 TeV ,” (2016).
- [5] M. Aaboud et al. (ATLAS), “Search for resonances in diphoton events at $\sqrt{s}=13 \text{ TeV}$ with the ATLAS detector,” (2016), 1606.03833.
- [6] V. Khachatryan et al. (CMS), “Search for resonant production of high-mass photon pairs in proton-proton collisions at $\sqrt{s} = 8$ and 13 TeV ,” (2016), 1606.04093.
- [7] A. Strumia (2016), 1605.09401, URL <http://inspirehep.net/record/1466435/files/arXiv:1605.09401.pdf>.
- [8] M. T. Arun and P. Saha, “Gravitons in multiply warped scenarios - at 750 GeV and beyond,” (2015), 1512.06335.
- [9] A. Falkowski and J. F. Kamenik, “Diphoton portal to warped gravity,” Phys. Rev. **D94**, 015008 (2016), 1603.06980.
- [10] C. Csaki and L. Randall, “A Diphoton Resonance from Bulk RS,” (2016), 1603.07303.
- [11] J. L. Hewett and T. G. Rizzo, “ 750 GeV Diphoton Resonance in Warped Geometries,” (2016), 1603.08250.
- [12] M. Dalchenko, B. Dutta, Y. Gao, T. Ghosh, and T. Kamon, “Exploring the Jet Multiplicity in the 750 GeV Diphoton Excess,” (2016), 1606.03067.
- [13] L. A. Harland-Lang, V. A. Khoze, M. G. Ryskin, and M. Spannowsky, “Jet activity as a probe of diphoton resonance production,” (2016), 1606.04902.
- [14] S. Fichtel, G. von Gersdorff, and C. Royon, “Scattering light by light at 750 GeV at the LHC,” Phys. Rev. **D93**, 075031 (2016), 1512.05751.
- [15] C. Csáki, J. Hubisz, and J. Terning, “Minimal model of a diphoton resonance: Production without gluon couplings,” Phys. Rev. **D93**, 035002 (2016), 1512.05776.
- [16] C. Csáki, J. Hubisz, S. Lombardo, and J. Terning, “Gluon versus photon production of a 750 GeV diphoton resonance,” Phys. Rev. **D93**, 095020 (2016), 1601.00638.
- [17] S. Abel and V. V. Khoze, “Photo-production of a 750 GeV di-photon resonance mediated by Kaluza-Klein leptons in the loop,” JHEP **05**, 063 (2016), 1601.07167.
- [18] S. Fichtel, G. von Gersdorff, and C. Royon, “Measuring the Diphoton Coupling of a 750 GeV Resonance,” Phys. Rev. Lett. **116**, 231801 (2016), 1601.01712.
- [19] A. Salvio, F. Staub, A. Strumia, and A. Urbano, “On the maximal diphoton width,” JHEP **03**, 214 (2016), 1602.01460.
- [20] N. D. Barrie, A. Kobakhidze, M. Talia, and L. Wu, “ 750 GeV Composite Axion as the LHC Diphoton Resonance,” Phys. Lett. **B755**, 343 (2016), 1602.00475.
- [21] N. D. Barrie, A. Kobakhidze, S. Liang, M. Talia, and L. Wu, “Heavy Leptonium as the Origin of the 750 GeV Diphoton Excess,” (2016), 1604.02803.
- [22] K. Ghosh, S. Jana, and S. Nandi, “Neutrino Mass Generation and 750 GeV Diphoton excess via photon-photon fusion at the Large Hadron Collider,” (2016), 1607.01910.
- [23] M. Cirelli, N. Fornengo, and A. Strumia, “Minimal dark matter,” Nucl. Phys. **B753**, 178 (2006), hep-ph/0512090.
- [24] P. Ko and T. Nomura, “ $SU(2)_L \times SU(2)_R$ minimal dark matter with $2 \text{ TeV } W'$,” Phys. Lett. **B753**, 612 (2016), 1510.07872.
- [25] R. N. Mohapatra and J. C. Pati, “Left-Right Gauge Symmetry and an Isoconjugate Model of CP Violation,” Phys. Rev. **D11**, 566 (1975).
- [26] G. Senjanovic and R. N. Mohapatra, “Exact Left-Right Symmetry and Spontaneous Violation of Parity,” Phys. Rev. **D12**, 1502 (1975).
- [27] R. N. Mohapatra and J. W. F. Valle, “Neutrino Mass and Baryon Number Nonconservation in Superstring Models,” Phys. Rev. **D34**, 1642 (1986).
- [28] S. M. Barr and I. Dorsner, “A Prediction from the type III see-saw mechanism,” Phys. Lett. **B632**, 527 (2006), hep-ph/0507067.
- [29] K. S. Babu and A. Patra, “Higgs Boson Spectra in Supersymmetric Left-Right Models,” Phys. Rev. **D93**, 055030 (2016), 1412.8714.
- [30] K. S. Babu, X.-G. He, and E. Ma, “New Supersymmetric Left-Right Gauge Model: Higgs Boson Structure and Neutral Current Analysis,” Phys. Rev. **D36**, 878 (1987).
- [31] E. Ma, “Particle Dichotomy and Left-Right Decomposition of $E(6)$ Superstring Models,” Phys. Rev. **D36**, 274 (1987).
- [32] G. Ecker, W. Grimus, and H. Neufeld, “Higgs Induced Flavor Changing Neutral Interactions in $SU(2)_L \times SU(2)_R \times U(1)$,” Phys. Lett. **B127**, 365 (1983), [Erratum: Phys. Lett. **B132**, 467 (1983)].
- [33] R. N. Mohapatra, G. Senjanovic, and M. D. Tran, “Strangeness Changing Processes and the Limit on the Right-handed Gauge Boson Mass,” Phys. Rev. **D28**, 546 (1983).
- [34] M. E. Pospelov, “FCNC in left-right symmetric theories and constraints on the right-handed scale,” Phys. Rev. **D56**, 259 (1997), hep-ph/9611422.
- [35] Y. Zhang, H. An, X. Ji, and R. N. Mohapatra, “General CP Violation in Minimal Left-Right Symmetric Model and Constraints on the Right-Handed Scale,” Nucl. Phys. **B802**, 247 (2008), 0712.4218.
- [36] A. Maiezza, M. Nemevsek, F. Nesti, and G. Senjanovic, “Left-Right Symmetry at LHC,” Phys. Rev. **D82**, 055022 (2010), 1005.5160.
- [37] E. Komatsu et al. (WMAP), “Seven-Year Wilkinson Microwave Anisotropy Probe (WMAP) Observations: Cosmological Interpretation,” Astrophys. J. Suppl. **192**, 18 (2011), 1001.4538.
- [38] P. A. R. Ade et al. (Planck), “Planck 2015 results. XIII. Cosmological parameters,” (2015), 1502.01589.
- [39] D. S. Akerib et al. (LUX), “First results from the LUX dark matter experiment at the Sanford Underground Research Facility,” Phys. Rev. Lett. **112**, 091303 (2014), 1310.8214.